

Boise State University
ScholarWorks

Geosciences Faculty Publications and Presentations

Department of Geosciences

1-1-2012

Partitioning of Rare Earth and High Field Strength Elements Between Titanite and Phonolitic Liquid

Paul H. Olin

Boise State University

John A. Wolff

Washington State University

NOTICE: This is the author's version of a work accepted for publication by Elsevier. Changes resulting from the publishing process, including peer review, editing, corrections, structural formatting and other quality control mechanisms, may not be reflected in this document. Changes may have been made to this work since it was submitted for publication. The definitive version has been published in *Lithos*, Volumes 128-131, 2012. DOI: [10.1016/j.lithos.2011.10.007](https://doi.org/10.1016/j.lithos.2011.10.007)

Partitioning of Rare Earth and High Field Strength Elements Between Titanite and Phonolitic Liquid

Paul H. Olin
Boise State University

John. A. Wolff
Washington State University

Abstract

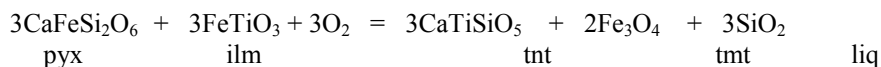
We present the results of a LA-ICPMS study of titanites and associated glasses from the mixed-magma phonolitic Fasnía Member of the Diego Hernández Formation, Tenerife, Canary Islands. We employ a method of identifying equilibrium mineral-melt pairs from natural samples using REE contents and a linear form of the lattice strain model equation (Blundy and Wood, 1994), where the Young's modulus (E_M) for the 7-fold coordinated site is an output variable. For felsic magmas that contain crystals potentially derived from a variety of environments within the system, this approach is more rigorous than the use of solely textural criteria such as mineral-glass proximity. We then estimate titanite/melt partition coefficients for Y, Zr, Nb, REE, Hf, Ta, U and Th. In common with prior studies, we find that middle REE partition more strongly into titanite than either light or heavy REE, and that REE partitioning behavior in titanite is reasonably predicted by the lattice strain model. Titanite also fractionates Y from Ho, Zr from Hf, and Nb from Ta. Comparison with experimental data indicates that melt structure effects on partitioning are significant, most particularly in very highly polymerized melts. We use the data to estimate 7-fold coordination radii for trivalent Pr, Nd, Ho, Tm and Lu, and to make approximate predictions of titanite/melt partitioning of Ra, Ac and Pa. Interpolation of data for heavy REE does not predict the behavior of Y, indicating that factors other than charge and radius are involved in partitioning. Variations in Y/Ho induced by magmatic processes appear to be negatively correlated with temperature, and are expected to be greatest in near-minimum melts.

Keywords: titanite, phonolitic magma, trace elements, partition coefficients, rare earth elements, high field strength elements

1. Introduction

Accessory phases in igneous and metamorphic rocks are valuable repositories of petrogenetic information. In igneous rocks, they are most commonly encountered in highly differentiated compositions such as rhyolites, trachytes, phonolites, and their plutonic equivalents. Many of them act as the principal sites for heavy elements that are normally present only in trace quantities in the whole rock, some of which (Sm-Nd, Lu-Hf plus U, Th and their decay products) may be employed as geochronometers on a variety of timescales. During igneous crystallization, these phases also exert strong compositional leverage on their host magmas, often leading to distinct, characteristic trace element signatures (Michael, 1983, 1988; Wolff and Storey, 1984; Cameron and Cameron, 1986). In addition, recent work has focused on the potential of Ti- and Zr-bearing accessory phases as geothermobarometers (Zack et al., 2004; Watson et al., 2006; Hayden et al., 2007).

Titanite (nominally CaTiSiO_5) is found as an accessory in high- $f\text{O}_2$ dacites and rhyolites and their plutonic equivalents (Lipman, 1971; Frost et al., 2000; Bachmann et al., 2005; Glazner et al., 2008). It is also stable in silica-undersaturated magmas at $f\text{O}_2 \leq \text{NNO}$, and is common in phonolites that lack ilmenite; a representative paragenesis in strongly differentiated magmas of low silica activity is therefore:



Titanite exhibits high values of the partition coefficient D [= (concentration in solid phase)/(concentration in liquid), C_s/C_l] for rare earth elements (REE) and high field strength elements (HFSE), and moreover a strong preference for middle REE over light and heavy REE, and for Ta over Nb (Wörner et al., 1983; Wolff, 1984; Green and Pearson, 1986, 1987; Tiepolo et al., 2002; Bachmann et al., 2005; Prowatke and Klemme, 2005). Fractionation of titanite during magmatic crystallization-differentiation therefore leaves a distinctive imprint of depletion in middle REE and increasing Nb/Ta in the residual liquid (Wolff, 1984; Wolff and Storey, 1984; Glazner et al., 2008). Partly because of the strong geochemical similarity of Nb and Ta, and the restricted stability in P - T - X space of Ti-phases such as titanite and rutile that exert strong leverage on these elements, variable Nb/Ta in different terrestrial reservoirs has been of particular interest (Green and Pearson, 1987; Rudnick et al., 1993; Green, 1995; Lundstrom et al., 1998; Barth et al., 2000; Horng and Hess, 2000; Tiepolo et al., 2000; Wade and Wood, 2001; Foley et al., 2002; John et al., 2010). Titanite also incorporates high concentrations of U and Th, and may be employed in geochronology (Frost et al., 2000).

Experimental data are available for titanite/melt element partitioning (Green and Pearson, 1986, 1987; Tiepolo et al., 2002; Prowatke and Klemme, 2005), but in all of these studies, non-natural compositions were employed to ensure measurable amounts of REE and HFSE (Green and Pearson, 1986, 1987) or crystallization of copious amounts of titanite (Tiepolo et al., 2002; Prowatke and Klemme, 2005). There is a shortfall of detailed information on titanite-melt partitioning of lithophile elements from natural samples, in particular from silica-undersaturated compositions. We know of no such studies more recent than Wörner et al. (1983) and Wolff (1984). In this paper, we present the results of a LA-ICPMS study of titanites and associated glasses from the phonolitic Fasnía Member of the Diego Hernández Formation, Tenerife, Canary Islands (Edgar et al., 2007). Following Olin and Wolff (2010), we employ a method of identifying equilibrium mineral-melt pairs from natural samples that is independent of textural context. We then present titanite/melt D values for Y, Zr, Nb, REE, Hf, Ta, Th and U and use the data to estimate 7-fold coordination radii for REE³⁺ not reported by Shannon (1976), and to approximately predict titanite/melt partitioning behavior of Ra, Ac and Pa. We then assess the results, paying particular attention to behaviors (melt structure effects, fractionation of cations of identical charge and radius) that are not predicted by the lattice strain model of Brice (1975) and Blundy and Wood (1994).

2. Samples and analytical methods

Titanites and glasses in this study come from the 309 ± 6 ka Fasnía Member phonolitic pumice deposit, Tenerife, Canary Islands. The Fasnía Member is one of the major units of the phonolitic, caldera-related Diego Hernández Formation of the Las Cañadas Upper Group on Tenerife (Edgar et al., 2007). Las Cañadas phonolites have whole-rock compositions that lie close to the 1 kbar water-saturated phonolitic minimum in the ne - ks - Q system (Hamilton and MacKenzie, 1965), oxygen fugacities close to the NNO buffer (Wolff and Storey, 1983) and temperatures typically in the range 790 – 850°C (Wolff and Storey, 1983; Bryan, 2006; Andújar et al., 2008). The phenocryst assemblage consists of sodic sanidine ± nepheline + haüyne + clinopyroxene + biotite + titanite + magnetite with trace amounts of apatite and pyrrhotite as inclusions in other minerals. This assemblage is consistent with equilibrium phase relations observed in the experiments on Diego Hernández phonolite by Andujar et al. (2008). The Fasnía Member is the product of the explosive eruption of ~13 km³ of phonolite magma with a large range in trace element abundances (Edgar et al., 2007), due to mixing of at least two distinct end member phonolites and a small volume of mafic magma that resulted in a dominant volume of hybrid phonolite (Olin, 2007). Despite variable trace element contents (Table 1), fresh Fasnía glasses considered here exhibit very little major element variation, with approximately 15 wt.% total alkalis and $(Na + K)/Al \approx 1$. The magmatic temperature is taken to be 825°C (Andujar et al., 2008).

Titanite occurs in small quantities ($\ll 1$ % modal abundance) in phonolitic pumices and in syenitic xenoliths in Fasnía deposits. It is distinctly straw yellow to yellow-orange in color. Small euhedral grains range in size from a few tens of microns to 0.5 mm; occasionally large (~1mm) composite grains are seen. Only euhedral grains were analyzed in this study.

The word ‘glass’ is used here to denote a single analysis of the vesicular glass in a polished section of a pumice clast. Glasses range in color from felsic to mafic and color does not necessarily correspond to bulk composition; for example, dark and light colored glasses might both have hybrid bulk compositions. Glasses were targeted throughout the deposit to capture the observed textural varieties of pumices as well as the wide compositional spectrum of the Fasnía.

The Fasnja samples are petrographically complex. Pre- and syn-eruptive chaotic mixing processes have scrambled magmatic components from at least three different end member magmas and a hybrid magma resulting in pumices throughout the deposit with varying degrees and styles of mingling and banding. Titanite and glasses in this study were sampled from throughout the Fasnja stratigraphy. We recognize that an inherent problem when dealing with natural samples from systems in which magma mixing has occurred is that no genetic relationships between mineral grains and enclosing or adjacent glasses can be assumed. Recent experiments by De Campos et al. (2011) have demonstrated that during a chaotic mixing event a highly heterogeneous magma body can be generated on short time and length scales; this process also mechanically separates minerals from their respective parental liquids. Although we employed petrographic textural analysis to reveal the complexity of the magma at the time of eruption via banded and mingled pumiceous samples, the utility of petrographic assessment of mineral-melt equilibrium is limited; this issue is further discussed, and a solution proposed, later in the paper.

All titanite and glass data reported here were generated in the Washington State University GeoAnalytical Laboratory using LA-ICP-MS analysis for trace element concentration determinations and the electron microprobe for major element analysis. Trace element concentrations in titanites and glasses were measured by ablating shallow (<5 μm deep) troughs with a New Wave 213 nm laser coupled to an Element2 high-resolution mass spectrometer operated in low resolution mode. For titanites, ablation troughs were 5 to 8 μm wide by 200 to 500 μm long. Grains were analyzed *in situ* where encountered in polished sections, but primarily as mineral separates mounted in epoxy. Trace element concentrations in pumiceous glasses were determined using LA-ICP-MS *in situ* on polished sections. Laser tracks were positioned to follow along bubble walls in pumice resulting in 5 to 8 μm -wide troughs with irregular geometries and lengths of 200 to 500 μm . For both titanites and glasses, acquired counts per second data were reduced offline and internally normalized to the electron microprobe determined SiO_2 contents and laser determined ^{29}Si counts per second. Two-point calibrations were constructed using BCR-2g and NIST 610 as standards. Gadolinium is not used in this study; there are unresolved issues with the ^{157}Gd isotope in many of the laser ablation analyses of both titanites and glasses.

Major and minor elements in titanites were measured using a Cameca electron microprobe in the Washington State University GeoAnalytical Laboratory. The instrument was operated at 15kv, using a spot diameter of ~4 microns and a beam current of 12nA. Zr and Nb are present in minor to major quantities in titanite and hence were analyzed by both methods.

Representative titanite and glass analyses are shown in Table 1; the complete titanite and glass data set for this study appears in electronic Appendix A.

3. Glass chemistry

The Fasnja phonolitic glasses exhibit a very limited range in major element geochemistry, consistent with minimum-melt compositions. However, they show a rather large range in trace element abundances due to mixing of at least two distinct end member phonolites (a 'low-Zr' and a 'high-Zr' phonolite) together with a small proportion of mafic magma to yield a dominant volume of hybrid phonolite (Olin, 2007). The low-Zr end member has slightly higher SiO_2 , CaO, and TiO_2 contents, but significantly lower incompatible trace elements (e.g., Rb, Zr) than the high-Zr end member. High-Zr phonolite is much more evolved than low-Zr phonolite, as indicated by higher incompatible element contents, strong MREE depletion (Fig. 1a), and higher Nb/Ta ratios. These features are consistent with a history of titanite fractionation observed in most Diego Hernández phonolites (Wolff and Storey, 1984; Wolff et al., 2000; Edgar et al., 2007). Hybrid phonolite values plot between high- and low-Zr end members for all elements and ratios (Fig 1a, Table 1).

4. Titanite chemistry

Fasnja titanites can be grouped into two types based on systematically different and highly variable REE and HFSE contents and ratios (Fig. 1b, Table 1). 'Low-Zr' titanites have lower Ti and HFSE contents, higher overall REE contents, and lower La/Sm and Nb/Ta ratios than 'high-Zr' titanites. High-Zr titanites have lower Ti contents, are depleted in MREE and have high Nb/Ta ratios. Ca and Al contents show no systematic differences between the two types, and Fe and F are slightly higher in high-Zr titanites than in low-Zr titanites. These variations are consistent with those seen in the glasses and can be explained by progressive fractional crystallization of titanite from phonolitic magma. It is clear that the two populations crystallized from different phonolitic liquids, and it is

reasonable to assign low-Zr titanites to a lower-Zr liquid than the high-Zr titanites. However, given 3 liquid populations but only 2 titanite types, confident matching of liquids and crystals is more difficult. The approach we use to identify cognate liquids for titanites is outlined below.

Some grains of both types of titanite show compositional zonation from core to rim, usually in a normal fashion (i.e., trace elements that are incompatible in the system as a whole, such as Zr, increase from core to rim). Jacketing of low-Zr by high-Zr compositions, and vice-versa, within a single grain is also seen, and may be due to crystal transfer between contrasting liquids (Olin, 2007). Grains showing compositional zoning are not rejected outright, rather rim analyses are included in the equilibrium assessment described below.

4.1. Cation substitutions

Titanite contains SiO₄ tetrahedra with groups of CaO₇ and TiO₆ polyhedra (Zachariassen, 1930). In addition to Ca, the irregular seven-coordination polyhedra (Speer and Gibbs, 1976) will accommodate Na, Sr, Ba, REE and Y. The octahedral site contains Ti, Al, Fe³⁺, Mg, Fe²⁺, Mn, Zr, Hf, Nb and Ta. Uranium and Th have ionic radii in octahedral coordination that are large for the Ti site, and fit better in the Ca site (Shannon, 1976). The Fasnja titanites contain significant Fe, but its degree of oxidation is unknown. However, the Tenerife phonolitic melts are predicted to be Fe³⁺-rich; Fe³⁺/Fe²⁺ is estimated at approximately 0.5 using MELTS (Ghiorso and Sack, 1995) hence Fe³⁺ was freely available during titanite growth. Cation site size considerations (see next section) strongly favor incorporation of Fe³⁺ over Fe²⁺ into titanite hence we make the assumption that all Fe in titanites is present as Fe³⁺.

In addition to ionic radius, coupled substitutions in titanite are constrained by the need to maintain charge balance and by the presence of OH⁻ and F⁻ (Sahama, 1946; Jaffe, 1947; Zabavnikova, 1957; Mongiorgi and Sanseverino, 1968; Cerny and Povondra, 1972; Higgins and Ribbe, 1976). In an environment rich in trace elements, additional substitutions are possible (Zabavnikova, 1957; Hollabaugh, 1980; Green and Pearson, 1986; Cerny et al., 1995; Tiepolo et al., 2002; Prowatke and Klemme, 2005), and numerous exchange reactions may control substitution of REE, HFSE, F, Na, Al and Fe³⁺ into titanite. Some possible substitutions, among others, are:

- i. (Al³⁺, Fe³⁺) + (OH⁻, F⁻) = Ti⁴⁺ + O²⁻
- ii. (Zr⁴⁺, Hf⁴⁺) = Ti⁴⁺
- iii. (Fe³⁺, Al³⁺) + (Nb⁵⁺, Ta⁵⁺) = 2 Ti⁴⁺
- iv. Na⁺ + (Nb⁵⁺, Ta⁵⁺) = Ca²⁺ + Ti⁴⁺
- v. (REE³⁺, Y³⁺) + (Fe³⁺, Al³⁺) = Ca²⁺ + Ti⁴⁺.

We find correlations between cations, and cations with F, suggesting that all these substitutions may operate to some extent. However, with the exception of substitution iii., all of the correlations have slopes inappropriate for the simple mechanism as written. The number of possible substitutions increases still further if there are vacancies within the structure. Prowatke and Klemme (2005) reviewed titanite data and substitution mechanisms with similar findings and concluded “matters appear to be... complicated.” Here, we assume that REE, Na, U and Th dominantly reside on the 7-coordinated Ca-site, and Zr, Hf, Nb, Ta, Al and Fe³⁺ on the octahedral Ti-site, hence an appropriate formula for Fasnja titanites is (Na⁺, Ca²⁺, Y³⁺, REE³⁺, Th⁴⁺, U⁴⁺) (Al³⁺, Fe³⁺, Ti⁴⁺, Zr⁴⁺, Hf⁴⁺, Nb⁵⁺, Ta⁵⁺) (SiO₄) (O²⁻, OH⁻, F⁻).

5. Partition coefficients

Numerous studies have successfully applied the LSM to mineral-melt partitioning, including experimental investigations of titanite growth from synthetic Ti-rich melts (Tiepolo et al., 2002; Prowatke and Klemme, 2005). In the lattice strain model (LSM) of Brice (1975) and Blundy and Wood (1994), the partition coefficient D_i at equilibrium of a cation with radius r_i entering a particular crystal lattice site M is given by

$$D_i = D_0 \cdot \exp\{-4\pi E_M N_A [r_0(r_i - r_0)^2/2 + (r_i - r_0)^3/3]/RT\} \quad (1)$$

where D_0 is the partition coefficient of an isoivalent ion of radius r_0 which enters the site without strain, E_M is the Young's modulus of site M, N_A is Avogadro's Number, R is the universal gas constant, and T is temperature in Kelvin. The relationship is most often plotted on an Onuma diagram as the logarithm of the partition coefficient versus ionic radius, producing a parabolic distribution (Fig. 2a). The partition coefficient D_0 for a cation with

optimal radius r_0 fixes the apex of the parabola, and its curvature is controlled by the Young's modulus (E_M) for the site. Larger E_M values 'tighten' the parabola, reflecting greater stiffness of the site and therefore a relatively narrower range of radii for cations that significantly substitute into the site. For the application of the model below, it is not necessary to know r_0 and D_0 *a priori* as long as there are enough elements to plot to define the shape of the parabola.

Before we can explore Fasnja titanite-melt partitioning, it is necessary to establish that the titanite grains and glasses used to obtain D values represent equilibrium pairs. Typically mineral-glass equilibrium is evaluated using grain shape and textural context; for example euhedral titanite grains appearing to be in textural equilibrium with the enclosing glass. However, in recent years it has become widely understood that despite passing all visual criteria for equilibrium, 'phenocrysts' in volcanic rocks are in many cases out of equilibrium with their enclosing glass or groundmass; the clearest evidence for this lies in contrasting radiogenic isotope ratios between crystals and groundmass (see Davidson et al., 2007, for a comprehensive review). In the absence of isotopic data, some other compositional criterion is therefore necessary to establish the identities of equilibrium mineral-melt pairs. Furthermore, in an ocean island such as Tenerife, lack of overall isotopic variation may in any case preclude the use of isotope ratios to identify mineral-melt equilibrium; isotopes may furthermore be susceptible to post-crystallization modification (Palacz and Wolff, 1989). As described above, magmatic processes have scrambled crystals and glasses in the compositionally variable Fasnja phonolite, precluding confident identification of mineral-glass pairs based on visual criteria. The method used by Olin and Wolff (2010) and outlined below is independent of major element mineral compositions, assumes that the LSM is a good first-order predictor of trace element partition coefficients, and does not rely on textural relationships.

For the 29 high-Zr titanite analyses, apparent D_{REE} values were calculated using LA-ICP-MS-determined concentrations of La, Ce, Sm, Tb, Dy, Er and Yb in the titanites and the approximately 570 phonolite glasses, including the low-Zr glasses which we would not predict to be in equilibrium with high-Zr titanites. Eu is omitted from this exercise due its unconstrained oxidation state, Pr, Nd, Ho, Tm and Lu are omitted because there is no ionic radius data reported for them in 7-fold coordination (Shannon, 1976), and Y is omitted because it does not behave as REE of similar radius (Olin and Wolff, 2010). Equilibrium between the high-Zr titanites and the different glasses is evaluated by assuming that isovalent cations entering a single lattice site will always follow a parabolic distribution in log D_i vs. r_i , using equation (1) rewritten as:

$$[RT/(-4\pi N_A)] * [\ln(D_i/D_0)] = E_M[r_0 * (r_i - r_0)^2/2 + (r_i - r_0)^3/3] \quad (2)$$

If the data follow the parabolic function exactly, the result is a straight line with slope E_M (Fig. 2b). Using equation (2) with the REE³⁺ indicated above, for each titanite analysis we chose to average the 5 paired glasses returning the best R^2 correlation coefficient for the linear regression, and thus represent the closest approach to equilibrium titanite-melt partition coefficients. Titanite-glass pairs with $R^2 < 0.90$ were rejected. During this exercise >16,000 possible high-Zr titanite-glass pairs were evaluated, and 139 titanite-glass pairs with $R^2 > 0.90$ were identified (see Appendix A). This approach is more rigorous than simply using predicted absolute D values because the fit does not depend on knowing D_0 or r_0 , and relies on multiple elements. We do not assume nor fit to any ^{VII}E³⁺ value, rather it is an output variable, being the slope of the linear form of the model equation (Fig. 2b). The results are that high-Zr titanites consistently return equilibrium matches with hybrid phonolite glass compositions, and are tightly grouped, as expected for mineral/melt pairs where neither exhibits large major-element compositional variation. No high-Zr titanite produced an equilibrium pair with either any high-Zr or low-Zr phonolite glasses. Low-Zr titanites return equivocal results and are not considered further here.

Partition coefficients determined for Fasnja high-Zr titanites are within the range of previously reported values (Fig. 2c, Table 2). Yttrium partitions less strongly than REE with similar ionic radii, imparting a distinct negative Y 'anomaly' to Onuma plots. This behavior is not predicted by the lattice strain model, and indicates that variables other than charge and radius are playing a discernable role in partitioning at magmatic temperatures.

The ^{VII}E³⁺ values returned in this study for identified equilibrium high-Zr titanite-glass pairs span approximately 50 GPa, with the median and average values nearly identical at 353 and 355 GPa, respectively (Table 2). This range in ^{VII}E³⁺ does not correlate with the R^2 correlation coefficient for the linear regression nor does it correlate markedly with any single geochemical parameter or element ratio. This suggests that ^{VII}E³⁺ may not have a constant value for high-Zr titanites in this system. Since cation site size is influenced by several physical and geochemical variables,

real variability in $^{VII}E^{3+}$ within a single system might reflect differences in physiochemical conditions in the hybrid magma, and the long-recognized irregularity of 7-fold coordinated Ca-site (Speer and Gibbs, 1976) could make titanite especially sensitive to subtle differences in magmatic conditions. Our highest $^{VII}E^{3+}$ value of 388 GPa (Table 2) is lower than the low values of 468 and 493 experimentally obtained by Tiepolo et al. (2002) and Prowatke and Klemme (2005), respectively, but from compositions quite different from ours.

6. Estimation of 7-fold coordination radii for trivalent Pr, Nd, Ho, Tm and Lu

Here we predict seven-fold coordinated ionic radii for REE^{3+} that are not reported by Shannon (1976). We do this by interpolation from REE with known radii for six-, seven-, and eight-fold coordination. From two linear regression equations for 7- vs. 6- and 7- vs. 8-fold radii, radii for cations with no reported 7-fold coordination value are calculated and averaged. These interpolated values are shown in Table 2 in italics, and are plotted as shaded circles in Fig 3c. Interpolated 7-fold values fall on or near the LSM model curve based on La, Ce, Sm, Tb, Dy, Er and Yb, and hence accurately predict the partitioning behavior of Pr, Nd, Ho, Tm and Lu.

7. Prediction of titanite/melt D_{Ra} , D_{Ac} and D_{Pa}

As a host for large cations including U and Th, titanite can potentially also accommodate their decay products. Interpretation of U,Th-decay series data from igneous rocks is aided by a knowledge of how decay products partition between minerals and melt. Here, we predict titanite/melt D values for Ra^{2+} , Ac^{3+} and Pa^{5+} . Results are given in Table 2.

We cannot calculate a LSM for divalent cations from analytical data because measured concentrations of Sr and Ba in titanite are too low to allow reliable estimation of D_{Sr} and D_{Ba} . Consequently, to estimate D_{Ra} , we equate D_0 and r_0 for divalent elements substituting on to the Ca site with D_{Ca} and r_{Ca} , and use the Hazen and Finger (1979) relationship $E \sim 1125Zd^{-3}$ (where Z = cation charge and d = cation-oxygen distance; Blundy and Wood, 1994, 2003). We estimate the 7-fold radius of Ra^{2+} as 1.44 Å. We find titanite/melt $D_{Ra} < 0.0001$.

Partitioning of Ac^{3+} is directly extrapolated using the LSM from the Onuma diagram for REE^{3+} , and an estimated 7-fold radius of 1.19 Å. The result $D_{Ac} = 0.30$ indicates that Ac is moderately incompatible into titanite, and likely significantly less compatible than either Th or U.

Protactinium is assumed to reside in magmas as Pa^{5+} . We assume that in titanite it resides wholly on the Ti site due to the large charge mismatch with the Ca site. Nb and Ta are close to the optimum size for substitution of pentavalent cations onto the Ti site in titanite, and, since $D_{Ta} > D_{Nb}$, we assume $D_0 = D_{Ta}$ and $r_0 = r_{Ta}$; E is again estimated from the Hazen and Finger (1979) relationship, which gives $D_{Pa} \sim 0.01D_{Ta}$, implying that D_{Pa} is close to unity. However, the Hazen and Finger (1979) relationship may considerably underestimate the 'stiffness' of small lattice sites (Blundy and Wood, 2003); for example if the actual value of E for this site is twice the calculated value, then $D_{Pa} \sim 0.01$. It is likely therefore that Pa is also incompatible in titanite, with $D_{Pa} \sim 1$ representing a maximum value for Fasnian titanites.

Although these estimates are approximate, we conclude that these decay-series products partition less strongly into titanite than their parents U and Th.

8. Influences on partitioning between titanite and melt

8.1. Mineral composition effects

The LSM predicts a dependency of D values on mineral composition. A change in the major cations occupying a particular site will shift the value of r_0 , raising the D values at constant r on the limb of the parabola that lies in the direction of the shift. A change in the size of one lattice site may in turn affect other sites in the same mineral. These effects are seen in minerals that exhibit major solid solutions; pyroxene is a good example (Wood and Blundy, 1997; Olin and Wolff, 2010). However most igneous titanite (and even titanites synthesized from compositions well outside the range of natural magmas, e.g. Prowatke and Klemme, 2005), is close to the ideal $CaTiSiO_4(O,OH,F)$ composition, and the r_0 values of the 7-coordinate Ca site and the octahedral Ti site are not expected to greatly vary. Nonetheless, some minor mineral compositional effects are apparent when our data are

compared with experimental results (Fig. 3). The clearest correlations are seen in Prowatke and Klemme's (2005) experiments, which were specifically designed to investigate melt composition effects on partitioning (see below), and in which the melt composition may have therefore influenced minor constituents in titanite such as Na and Al, in addition to REE and HFSE. Overall, we found no clear correlation between other cations substituting in the Ca- and Ti-sites respectively versus REE ratios and Nb/Ta. There does however appear to be an overall negative correlation between D_{Zr}/D_{Hf} and Al/Ti (Fig. 3a), consistent with a slightly smaller cation radius of Hf than Zr (Shannon, 1976). There is no such relation between D_{Nb}/D_{Ta} and Al/Ti (Fig. 3b).

8.2. Melt structural effects

Despite the success of the LSM in predicting partition coefficients (Blundy and Wood, 2001), it has long been recognized that melt composition may exert an influence on mineral/melt partitioning (Watson, 1976; Ryerson and Hess, 1978; Ponader and Brown, 1989; Schmidt et al., 2004, 2006). A phase such as titanite, which precipitates from a variety of melt compositions but does not itself vary strongly in composition, is useful for isolating the effects of melt composition and structure on mineral/melt trace element partitioning. This was explicitly addressed by Prowatke and Klemme (2005), whose anhydrous experiments were designed to achieve titanite saturation across a wide variety of melt compositions as measured by the alumina saturation index ($Al_2O_3/(Na_2O + K_2O + CaO)$). Prowatke and Klemme (2005) found a strong positive correlations between alumina saturation and titanite/melt partitioning of REE, Th, Nb and Ta, confirming the predictions of Watson (1976) and Ryerson and Hess (1978) that highly polymerized melts will tend to reject highly charged cations such as REE and HFSE. We have therefore compared our results with those of Prowatke and Klemme (2005) and the hydrous experiments of Green and Pearson (1986, 1987) and Tieplo et al. (2002). We use the ratio of non-bridging oxygens to tetrahedrally coordinated cations (NBO/T) in preference to the alumina saturation index as a measure of melt polymerization, because it is calculated from the entire melt composition. This is important because, in addition to water, our melts and those of Green and Pearson (1986, 1987) and Tiepolo et al. (2002) contain significant amounts of iron. We find that while the partitioning behavior of REE and HFSE show good correlations with NBO/T for Prowatke and Klemme's (2005) highly polymerized melts, there is little correlation among the other studies. This is well shown in a plot of apparent E_{VII} vs. NBO/T (Fig. 4a) where a distinct break occurs at NBO/T \sim 0.25, with more weakly polymerized melts exerting no influence on titanite/melt partitioning of REE, whereas melt composition to a large degree controls the REE at NBO/T < 0.25. Similarly, D_{Zr}/D_{Hf} and D_U/D_{Th} are only correlated with NBO/T at the low values of the latter obtained in Prowatke and Klemme's (2005) experiments. Also, there is a clear break in D_{Nb}/D_{Ta} at NBO/T \sim 0.25, with markedly greater titanite-melt fractionation of Nb and Ta found in Prowatke and Klemme's (2005) six most highly polymerized melts (Fig. 4b).

Changing melt composition and hence melt structure influences the coordination environment of cations and will in turn influence mineral-melt cation partitioning. From a petrologic standpoint, the question is whether or not these effects are subordinate to solid-phase chemistry in predicting D values. The data summarized in Fig. 4 suggest that melt structure effects may have a significant influence on mineral/melt trace element partitioning in water-poor, metaluminous to peraluminous silicic magmas with low NBO/T, but less so in water-bearing, metaluminous to peralkaline silicic melts and mafic melts with higher NBO/T. This is broadly consistent with evidence from calorimetry and viscosity measurements for a fundamental change in melt structure at the transition from metaluminous to peraluminous compositions (Webb et al., 2004; Webb, 2005, 2008; although not all of the compositions with NBO/T < 0.25 in Fig. 4 are peraluminous, a direct comparison of melts in the titanite partitioning experiments with the results of Webb and co-workers is not possible due to the presence of significant TiO_2 , FeO^* and MgO in addition to SiO_2 , Al_2O_3 , CaO , Na_2O and K_2O). Most natural silicic melts are typically water-rich and thus have higher NBO/T than their anhydrous equivalents; consequently melt compositional effects may be subordinate to mineral chemistry across most of the spectrum of igneous compositions (Fig. 4).

8.3. Factors other than cation charge and radius: Y/Ho, Zr/Hf, Nb/Ta

The elements in each of these pairs have closely similar radii and have been viewed in the past as chemically near-identical at magmatic temperatures. Thus, Y was commonly used as a proxy for the HREE between Tb and Yb prior to the routine availability of high-quality ICPMS data for all 14 REE (for example, Thompson et al., 1984). Significant fractionation in these pairs of elements is observed at sub-magmatic temperatures (Bau, 1996, 1999; Bau and Dulski, 1999) and, in plutonic rocks, has been ascribed to the action of aqueous fluids during the final stages of crystallization (Irber, 1999). Carbonatite liquids have also been implicated in Zr/Hf and Nb/Ta fractionation

(Rudnik et al., 1993). Nonetheless, it is now well established that these element pairs are fractionated during crystallization-differentiation of silicate magmas (e.g., Tiepolo et al., 2001).

The ability of the LSM to predict these fractionations depends on accurate ionic radius data. Nb^{5+} and Ta^{5+} are conventionally viewed as having identical radii, Zr^{4+} and Hf^{4+} are slightly different, while the radius of Y^{3+} lies between those of Dy^{3+} and Ho^{3+} in eight-fold coordination, but is nearly identical to Ho^{3+} in 6-fold coordination; our interpolated radius for Ho^{3+} in 7-fold coordination is almost identical to the tabulated value for Y^{3+} (Table 2). Accuracy of the LSM is difficult to assess for the pairs Nb-Ta and Zr-Hf, because the high E values associated with high valencies imply easily detectable changes in D at variations in $r \leq 0.01$ Å, beyond the resolution of the Shannon (1976) ionic radius data. Based on $D_{\text{Nb}}/D_{\text{Ta}}$ variations in Ti-pargasite and kaersutite documented by Tiepolo et al. (2000), they and Blundy and Wood (2003) in fact propose that the ionic radius of Ta^{5+} is 0.01 – 0.02 Å smaller than that of Nb^{5+} . Olin and Wolff (2010) however showed that Y^{3+} cpx/melt partitioning deviates from that of the HREE to an extent that the LSM cannot explain unless the Shannon (1976) value of the ionic radius for Y^{3+} is grossly in error. Fasnja titanite displays similar behavior to a greater degree (Figs. 2, 3, 6), and the same effect is also seen in the experimental data of Tiepolo et al. (2002). Although small differences in ionic radius may indeed cause fractionation of Nb from Ta and Zr from Hf, this cannot explain the fractionation of Y from the heavy REE. Thermodynamic data for rare earth oxides (Jacobson, 1989) indicate that larger energy changes are associated with substituting Y for Ho at magmatic temperatures than for exchanging neighboring heavy REE (Dy, Er) for Ho; put simply, Y is not a lanthanide element and should not be expected to behave exactly like one. The pairs Y-Ho, Zr-Hf and Nb-Ta share a common feature, which is that the lighter cation has the outer electronic configuration [Kr], and the heavier cation has buried 4f electrons and the outer electronic configuration [Xe]. Contrasts in behavior between the members of each pair may therefore be due to electronic effects and/or mass effects as discussed by Olin and Wolff (2010).

Regardless of the fundamental causes of the effect, element fractionations are in general expected to be more marked at lower temperatures, as noted by Bau (1996, 1999), Bau and Dulski (1999) and Irber (1999); these effects are nonetheless significant within the range of silicate magma temperatures. Of the available experimental titanite/melt data, three of the four 850°C experiments reported by Tiepolo et al. (2002) show a significant lowering of D_Y from its expected value, while none of the 1150°C experiments reported by Prowatke and Klemme (2005) show the effect. This apparent temperature dependence of mineral/melt D_Y/D_{Ho} is also seen in the pyroxene partitioning data (Fig. 5); the effect appears to become negligible at about 1200°C. This in turn suggests the possible use of Y/Ho ratios as a geochemical tracer of low-temperature melting (below ~1100°C) processes in petrogenesis and magma source history; however, incorporation of sediment into magma sources could have similar effects due to the strong fractionation of Y from Ho in the marine environment (Kawabe et al., 1991; Nozaki et al., 1997).

9. Conclusions

Titanite/melt partitioning behavior for Y, Zr, Nb, REE, Hf, Ta, U and Th in the Fasnja member phonolite is broadly similar to that documented in experimental studies, with middle REE partitioning more strongly into titanite than either light or heavy REE. The partitioning behavior of REE^{3+} for which sevenfold coordination radii are not listed by Shannon (1976) is accurately predicted by interpolation from sixfold and eightfold ionic radii. Intermediate products of actinide decay series of geologic interest (Ra, Ac and Pa) are predicted to partition into titanite less strongly than U and Th. Melt structure effects on partitioning appear to be significant for very highly polymerized melts ($\text{NBO}/\text{T} \leq 0.3$) such as dry, metaluminous to peraluminous rhyolites, but less so for the majority of natural melt compositions. Fasnja titanite fractionates Y from Ho, Zr from Hf, and Nb from Ta. In particular, interpolation of data for heavy REE does not predict the behavior of Y, indicating that factors other than charge and radius are involved in partitioning. Variations in Y/Ho induced by magmatic processes appear to be negatively correlated with temperature, and are expected to be most significant in near-minimum (i.e. rhyolitic and phonolitic) melts.

Acknowledgements

We thank Charles Knaack and Scott Cornelius of the Washington State University GeoAnalytical Laboratory for their assistance with LA-ICPMS and electron microprobe data collection. Fieldwork on Tenerife was funded by NSF grant EAR-0001013. We also thank Gerhard Wörner and other reviewers for their thoughtful and constructive comments.

References

- Andujar J., Costa, F., Martí, J., Wolff, J.A., Carroll, M.R., 2008. Experimental constraints on pre-eruptive conditions of phonolitic magma from the caldera-forming El Abrigo eruption, Tenerife (Canary Islands). *Chemical Geology* 257, 173-191.
- Bachmann, O., Dungan, M.A., Bussy, F., 2005. Insights into shallow magmatic processes in large silicic magma bodies: the trace element record in the Fish Canyon magma body, Colorado. *Contributions to Mineralogy and Petrology* 43, 1469-1503, doi:10.1007/s00410-005-0653-z.
- Barth, M.G., McDonough, W.F., Rudnick, R.L., 2000. Tracking the budget of Nb and Ta in the continental crust. *Chemical Geology* 165, 197-213.
- Bau, M., 1996. Controls on the fractionation of isovalent trace elements in magmatic and aqueous systems: evidence from Y/Ho, Zr/Hf, and lanthanide tetrad effect. *Contributions to Mineralogy Petrology* 123, 323-333.
- Bau, M., 1999. Scavenging of dissolved yttrium and rare earths by precipitating iron oxyhydroxide: Experimental evidence for Ce oxidation, Y-Ho fractionation, and lanthanide tetrad effect. *Geochimica et Cosmochimica Acta* 63, 67-77.
- Bau, M., Dulski, P., 1999. Comparing yttrium and rare earths in hydrothermal fluids from the Mid-Atlantic Ridge: Implications for Y and REE behavior during near-vent mixing and for the Y/Ho ratio of Proterozoic seawater. *Chemical Geology* 155, 77-79.
- Blundy, J., Wood, B., 2003. Partitioning of trace elements between crystals and melts. *Earth and Planetary Science Letters* 210, 383-397.
- Blundy, J., Wood, B., 1994. Prediction of crystal-melt partition coefficients from elastic moduli. *Nature* 372, 452-454.
- Brice, J.C., 1975. Some thermodynamic aspects of the growth of strained crystals. *Journal of Crystal Growth* 28, 249-253.
- Bryan, S.E., 2006. Petrology and geochemistry of the Quaternary caldera-forming phonolitic Granadilla eruption, Tenerife (Canary Islands). *Journal of Petrology* 47, 1557-1598.
- Cameron, K.L., Cameron, M., 1986. Whole rock/groundmass differentiation trends of rare earth elements in high-silica rhyolites. *Geochimica et Cosmochimica Acta* 50, 759-770.
- Cérvny, P., Povondra, P., 1972. An Al, F-rich metamict titanite from Czechoslovakia. *Neues Jahrbuch für Mineralogie - Monatshefte* 9, 400-406.
- Cérvny, P., Novak, M., Chapman, R., 1995. The Al(Nb)TaTi-2 substitution in titanite: the emergence of a new species? *Mineralogy and Petrology* 52, 61-73.
- Davidson, J.P., Morgan, D.J., Charleir, B.L.A., Harlou, R., Hora, J.M., 2007. Microsampling and isotopic analysis of igneous rock: implications for the study of magmatic systems. *Annual Reviews of Earth and Planetary Sciences* 35, 273-311.
- De Campos, C.P., Perugini, D., Ertel-Ingrisch, W., Dingwell, D.B., Poli, G., 2011. Enhancement of magma mixing efficiency by chaotic dynamics: an experimental study. *Contributions to Mineralogy and Petrology* 161, 863-881, doi:10.1007/s00410-010-0569-0.
- Edgar, C., Wolff, J.A., Olin, P.H., Nichols, H.J., Pitarri, A., Cas, R.A.F., Reiners, P.W., Spell, T.L., Martí, J., 2007. The late Quaternary Diego Hernandez Formation, Tenerife: a cycle of repeated voluminous explosive phonolitic eruptions. *Journal of Volcanology and Geothermal Research* 160, 59-85.
- Frost, B.R., Chamberlain, K.R., Schumaker, J.C., 2000. Sphene (titanite): phase relations and role as a geochronometer. *Chemical Geology* 172, 131-148.
- Foley, S.F., Tiepolo, M., Vannucci, R., 2002. Growth of early continental crust controlled by melting of amphibolite in subduction zones. *Nature* 417, 837-840, doi:10.1038/nature00799.
- Ghiorso, S., Sack, R.O., 1995. Chemical mass transfer in magmatic processes. IV. A revised and internally consistent thermodynamic model for the interpolation and extrapolation of liquid-solid equilibria in magmatic systems at elevated temperatures and pressures. *Contributions to Mineralogy and Petrology* 119, 197-212.
- Glazner, A.F., Coleman, D.S., Bartley, J.M., 2008. The tenuous connection between high-silica rhyolites and granodiorite plutons. *Geology* 36, 183-186.
- Green, T.H., 1995. Significance of Nb/Ta as an indicator of geochemical processes in the crust-mantle system. *Chemical Geology* 120, 347-359.
- Green, T.H., Pearson, N.J., 1986. Rare-earth element partitioning between sphene and co-existing silicate liquid at high pressure and temperature. *Chemical Geology* 55, 105-119.

- Green, T.H., Pearson, N.J., 1987. An experimental study of Nb and Ta partitioning between Ti-rich minerals and silicate liquids at high pressure and temperature. *Geochimica et Cosmochimica Acta* 51, 55-62.
- Hamilton, D.L., MacKenzie, W.S., 1965. Phase-equilibrium studies in the system $\text{NaAlSi}_3\text{O}_8$ (nepheline) – KAlSi_3O_8 (kalsilite) – SiO_2 – H_2O . *Mineralogical Magazine* 34, 214-231.
- Hayden, L.A., Watson, E.B., Wark, D.A., 2007. A thermobarometer for sphene (titanite). *Contributions to Mineralogy and Petrology* 155, 529-540.
- Hazen, R.M., Finger, L.W., 1979. Bulk modulus-volume relationship for cation-anion polyhedra. *Journal of Geophysical Research* 84, 6723-6728.
- Higgins, J.B., Ribbe, P.H., 1976. The crystal chemistry and space groups of natural and synthetic titanites. *American Mineralogist* 62, 878-888.
- Hollabaugh, C.L., 1980. Experimental mineralogy and crystal chemistry of sphene in the system soda-lime-alumina-titanium-silica-water. Ph.D. Thesis, Washington State University, 107 pp.
- Hornig, W., Hess, P.C., 2000. Partition coefficients of Nb and Ta between rutile and anhydrous haplogranite melts. *Contributions to Mineralogy and Petrology* 138, 176-185.
- Irber, W., 1999. The lanthanide tetrad effect and its correlation with K/Rb, Eu/Eu^* , Sr/Eu, Y/Ho, and Zr/Hf of evolving peraluminous granite suites. *Geochimica et Cosmochimica Acta* 63, 489-508.
- Jacobson, N.S., 1989. Thermodynamic properties of some metal oxide-zirconia systems. NASA Technical Memorandum 102351, 62 pp.
- Jaffe, H.W., 1947. Reexamination of sphene (titanite). *American Mineralogist* 32, 637-642.
- John, T., Klemm, R., Klemme, S., Pfänder, J.A., Hoffman, J.E., Gao, J., 2010. Nb-Ta fractionation by partial melting at the titanite-rutile transition. *Contributions to Mineralogy and Petrology* 161, 35-45, doi:10.1007/s00410-010-0520-4.
- Kawabe, I., Kitahara, Y., Naito, K., 1991. Non-chondritic yttrium/holmium ratio and lanthanide tetrad effect observed in pre-Cenozoic limestones. *Geochemical Journal* 25, 31-44.
- Lipman, P.W., 1971. Iron-titanium oxide phenocrysts in compositionally zoned ash-flow sheets from southern Nevada. *Journal of Geology* 79, 438-456.
- Lundstrom, C.C., Shaw, H.F., Ryerson, F.J., Williams, Q., Gill, J., 1998. Crystal chemical control of clinopyroxene-melt partitioning in the Di-Ab-An system: implications for elemental fractionations in the depleted mantle. *Geochimica et Cosmochimica Acta* 62, 2849-2862.
- McDonough, W.F., Sun, S.-S., 1995. Composition of the Earth. *Chemical Geology* 120, 223-253.
- Michael, P.J., 1988. Partition coefficients for rare earth elements in mafic minerals of high silica rhyolites: The importance of accessory mineral inclusions. *Geochimica et Cosmochimica Acta* 52, 275-282.
- Michael, P.J., 1983. Chemical differentiation of the Bishop Tuff and other high-silica magmas through crystallization processes. *Geology* 11, 31-34.
- Mongiorgi, R., Sanseverino, L.R. di, 1968. A reconsideration of the structure of titanite, CaTiOSiO_5 . *Mineralogica et Petrographica Acta* 14, 123-141.
- Ni, H., Behrens, H., Zhang, Y., 2009. Water diffusion in dacitic melt. *Geochimica et Cosmochimica Acta* 73, 3642-3655.
- Nozaki, Y., Zhang, J., Amakawa, H., 1997. The fractionation between Y and Ho in the marine environment. *Earth and Planetary Science Letters* 148, 329-340.
- Olin, P.H., 2007. Magma dynamics of the Diego Hernández Formation, Tenerife, Canary Islands. PhD thesis, Washington State Univ, USA, 416 pp.
- Olin, P.H., Wolff, J.A., 2010. Rare earth and high field strength element partitioning between iron-rich clinopyroxenes and felsic liquids. *Contributions to Mineralogy and Petrology* 160, 761-775, doi:10.1007/s00410-010-0506-2.
- Palacz, Z.A., Wolff, J.A., 1989. Strontium, neodymium and lead isotope characteristics of the Granadilla Pumice, Tenerife: a study of the causes of strontium isotope disequilibrium in felsic pyroclastic deposits. *Geological Society Special Publication* 42, 147-159.
- [Ponader, C.W., Brown, Jr., G.E., 1989.](#)
- Prowatke, S., Klemme, S., 2005. Effect of melt composition on the partitioning of trace elements between titanite and silicate melt. *Geochimica et Cosmochimica Acta* 69, 695-709.
- Rudnick, R.L., McDonough, W.F., Chappell, B.W., 1993. Carbonatite metasomatism in the northern Tanzanian mantle; petrographic and geochemical characteristics. *Earth and Planetary Science Letters* 114, 463-475.
- Ryerson, F.J., Hess, P.C., 1978. Implications of liquid-liquid distribution coefficients to mineral-liquid partitioning. *Geochimica et Cosmochimica Acta* 42, 921-932.

- Sahama, T.G., 1946. On the chemistry of the mineral titanite. *Bulletin de la Commission Geologique de Finland* 138, 88-120.
- Shannon, R.D., 1976. Revised effective ionic radii and systematic studies of interatomic distances in halides and chalcogenides. *Acta Crystallographica A* 32, 751-767.
- Sowerby, J.R., Keppeler, H., 1999. Water speciation in rhyolitic melt determined by in-situ infrared spectroscopy. *American Mineralogist* 84, 1843-1849.
- Speer, J.A., Gibbs, G.V., 1976. The crystal structure of synthetic titanite, CaTiOSiO_4 , and the domain textures of natural titanites. *American Mineralogist* 61, 238-247.
- Starkel, W.A., 2008. Petrologic comparison of the West Bennett Hills rhyolites to the central Snake River Plain rhyolites. MS thesis, Washington State Univ, USA, 244 pp.
- Thompson, R.N., Morrison, M.A., Hendry, G.L., Parry, S.J., 1984. An assessment of the relative roles of crust and mantle in magma genesis: an elemental approach. *Philosophical Transactions of the Royal Society of London A* 310, 549-590.
- Tiepolo, M., Oberti, R., Vannucci, R., 2002. Trace-element incorporation in titanite: constraints from experimentally determined solid/liquid partition coefficients. *Chemical Geology* 191, 105-119.
- Tiepolo, M., Bottazzi, P., Foley, S., Oberti, R., Vannucci, R., Zanetti, A., 2001. Fractionation of Nb and Ta from Zr and Hf at mantle depths: the role of titanian pargasite and kaersutite. *Journal of Petrology* 42, 221-231.
- Tiepolo, M., Vannucci, R., Oberti, R., Foley, S., Bottazzi, P., Zanetti, A., 2000. Nb and Ta incorporation and fractionation in titanian pargasite and kaersutite: crystal-chemical constraints and implications for natural systems. *Earth and Planetary Science Letters* 176, 185-200.
- Wade, J., Wood, B.J., 2001. The Earth's 'missing' Nb may be in the core. *Nature* 409, 75-78.
- Watson, E.B., 1976. Two-liquid partition coefficients: experimental data and geochemical implications. *Contributions to Mineralogy and Petrology* 56, 119-134.
- Watson, E.B., Wark, D.A., Thomas, J.B., 2006. Crystallization thermometers for zircon and rutile. *Contributions to Mineralogy and Petrology* 151, 413-433.
- Wolff, J.A., 1984. Variation in Nb/Ta during differentiation of phonolitic magma, Tenerife, Canary Islands. *Geochimica et Cosmochimica Acta* 48, 1345-1348.
- Wolff, J.A., Grandy, J.S., Larson, P.B., 2000. Interaction of mantle-derived magma with island crust? Trace element and oxygen isotope data from the Diego Hernandez Formation, Las Cañadas, Tenerife. *Journal of Volcanology and Geothermal Research* 103, 343-366.
- Wolff, J.A., Storey, M., 1983. The volatile component of some pumice-forming alkaline magmas from the Azores and Canary Islands. *Contributions to Mineralogy and Petrology* 82, 66-74.
- Wolff, J.A., Storey, M., 1984. Zoning in highly alkaline magma bodies. *Geological Magazine* 121, 563-575.
- Wood, B.J., Blundy, J.D., 2001. The effect of cation charge on crystal-melt partitioning of trace elements. *Earth and Planetary Science Letters* 188, 59-71.
- Wood, B., Blundy, J., 1997. A predictive model for rare earth element partitioning between clinopyroxene and anhydrous silicate melt. *Contributions to Mineralogy and Petrology* 129, 166-181.
- Wörner, G., Beusen, J.M., Duchateau, N., Gijbels, R., Schmincke, H.-U., 1983. Trace element abundances and mineral/melt distribution coefficients in phonolites from the Laacher See Volcano (Germany). *Contributions to Mineralogy and Petrology* 84, 152-173.
- Zabavnikova, I.I., 1957. Diadochic substitution in sphene. *Geochemistry* 3, 271-278
- Zachariasen, W.H., 1930. The crystal structure of titanite. *Zeitschrift für Kristallographie* 73, 7-16.
- Zack, T., Moraes, R., Kronz, A., 2004. Temperature dependence of Zr in rutile: empirical calibration of a rutile thermometer. *Contributions to Mineralogy and Petrology* 148, 471-488.

Figure captions

Figure 1. Rare earth element + Y contents of **A.** Fasnja titanites and **B.** glasses, normalized to bulk silicate earth (BSE; McDonough and Sun, 1995).

Figure 2. **A.** Lattice strain model plotted as Log (partition coefficient) versus ionic radius for idealized elements of the same valence state and coordination number, where D_0 is the partition coefficient for the optimal ionic radius r_0 , and E_M is the Young's modulus for the site. **B.** Average of best-fit D_{REE} values for high-Zr titanite, plotted according to eqn. (2) to illustrate the method of finding equilibrium titanite-glass pairs. **C.** Average best-fit D_{REE} values for titanite glass pairs in the Fasnja Member (FM) compared with previous studies.

Figure 3. High field strength element partition coefficient ratios vs. Al/Ti in titanite: **A.** D_{Zr}/D_{HF} ; **B.** D_{Nb}/D_{Ta} , for our data and the experimental results of Green and Pearson (1987), Tiepolo et al. (2002) and Prowatke and Klemme (2005).

Figure 4. **A.** $E_{VII,REE}$ and **B.** D_{Nb}/D_{Ta} vs. NBO/T for our data and the experimental results of Green and Pearson (1986, 1987), Tiepolo et al. (2002) and Prowatke and Klemme (2005). $E_{VII,REE}$ is used in this plot as a measure of overall REE partitioning behavior. $NBO/T = (2O + 4T)/T$, where O = total oxygen atoms and T = (Si + Al + Fe³⁺ + Ti) on a molar basis. This requires assumptions about the speciation of water, since only dissociated H₂O is assumed to contribute to NBO/T. Speciation depends on several variables including temperature, melt composition and total water content (Sowerby and Keppler, 1999; Ni et al., 2009). Here, we assume that water is fully dissociated at total melt water contents of 3.0 wt. %, at which concentration the melt is saturated in OH⁻. This assumption is conservative in that while allowing for the effect of water content, it has the effect of limiting the calculation of very high NBO/T values. Water contents are given by Tiepolo et al. (2002), and are estimated by difference from the microprobe glass analyses of Green and Pearson (1986, 1987); Fasnja value from Olin and Wolff (2010).

Figure 5. Mineral/melt D_Y/D_{Ho} vs. temperature for clinopyroxene and titanite. Clinopyroxene-temperature data from Andujar (2008) and Starkel (2008); titanite-temperature data from Andujar (2008), Tiepolo et al. (2002) and Prowatke and Klemme (2005). Neither of the latter two studies presents Ho data; D_{Ho} was interpolated from other heavy REE.

Table 1 - Representative Fasnja Member titanite and glass analyses

| | high-Zr titanite | low-Zr titanite | low-Zr phonolite | hybrid phonolite | high-Zr phonolite |
|--------------------------------|------------------|-----------------|------------------|------------------|-------------------|
| EM# | 99-6_3_1 | 99-6_5_1 | 99TF8Dc | 00TF171W | 99TF8Dr |
| LAICPMS# | 99TF6sphB_sph3b | 99TF6sphB_sph5r | 99TF8D_11 | 00TF171W16 | 99TF8D_1 |
| wt% SiO ₂ | 29.14 | 29.85 | 59.11 | 57.89 | 58.07 |
| Al ₂ O ₃ | 1.04 | 1.04 | 19.64 | 21.32 | 22.09 |
| TiO ₂ | 32.95 | 36.53 | 0.92 | 0.34 | 0.30 |
| FeO | 1.88 | 1.37 | 2.86 | 2.28 | 2.32 |
| MnO | 0.12 | 0.12 | 0.13 | 0.20 | 0.21 |
| MgO | 0.02 | 0.05 | 0.52 | 0.24 | 0.16 |
| CaO | 26.68 | 26.44 | 1.38 | 0.75 | 0.58 |
| Na ₂ O | 0.12 | 0.04 | 7.16 | 8.21 | 10.02 |
| K ₂ O | n.d. | n.d. | 5.91 | 5.47 | 5.88 |
| ZrO ₂ | 1.81 | 0.53 | n.d. | n.d. | n.d. |
| Nb ₂ O ₅ | 1.55 | 0.79 | n.d. | n.d. | n.d. |
| F | 0.64 | 0.13 | n.d. | n.d. | n.d. |
| SUM | 95.95 | 96.91 | 97.63 | 96.69 | 99.64 |
| ppm Y | 867 | 1,882 | 27 | 24 | 31 |
| Zr | 13,632 | 4,197 | 607 | 1,730 | 2,617 |
| Nb | 10,362 | 5,771 | 211 | 255 | 301 |
| La | 3,299 | 2,997 | 100 | 101 | 133 |
| Ce | 5,572 | 7,773 | 189 | 100 | 138 |
| Pr | 555 | 1,082 | 16.9 | 7.6 | 9.0 |
| Nd | 1,736 | 4,655 | 59 | 21 | 23 |
| Sm | 250 | 872 | 9.08 | 3.03 | 3.26 |
| Eu | 41 | 176 | 2.46 | 0.51 | 0.42 |
| Gd | 212 | 681 | n.d. | n.d. | n.d. |
| Tb | 28 | 93 | 0.96 | 0.39 | 0.50 |
| Dy | 165 | 467 | 4.9 | 2.5 | 3.8 |
| Ho | 32 | 79 | 1.09 | 0.71 | 0.96 |
| Er | 86 | 178 | 2.6 | 2.3 | 3.4 |
| Tm | 11 | 20 | 0.34 | 0.42 | 0.72 |
| Yb | 68 | 107 | 2.9 | 2.9 | 5.5 |
| Lu | 7.2 | 10.9 | 0.34 | 0.54 | 0.94 |
| Hf | 407 | 125 | 11 | 29 | 42 |
| Ta | 796 | 827 | 12 | 7 | 7 |
| Pb | 1.01 | 0.56 | 12 | 20 | 37 |
| Th | 98 | 102 | 17 | 48 | 77 |
| U | 17.0 | 8.0 | 5.3 | 11.3 | 21.0 |

LAICPMS precision reported in Appendix A

Table 2 - Partition coefficients, ionic radii & model values

| | Maximum | Minimum | Median | Average | 2 sigma | Model value | 7-fold ionic radius (Å) |
|-------------------------------|---------|---------|--------|---------|---------|-------------|-------------------------|
| D_Y | 36 | 25 | 31 | 30 | 5 | 47 | 0.960 |
| D_{Zr} | 10 | 5.2 | 7 | 7 | 2 | n.d. | |
| D_{Nb} | 43 | 32 | 36 | 36 | 6 | n.d. | |
| D_{La} | 29 | 21 | 25 | 25 | 5 | 24 | 1.100 |
| D_{Ce} | 48 | 34 | 39 | 40 | 7 | 47 | 1.070 |
| D_{Pr} | 67 | 47 | 55 | 55 | 9 | 56 | 1.058 |
| D_{Nd} | 81 | 52 | 63 | 63 | 13 | 64 | 1.046 |
| D_{Sm} | 89 | 59 | 72 | 72 | 15 | 74 | 1.020 |
| D_{Tb} | 79 | 51 | 62 | 62 | 14 | 61 | 0.980 |
| D_{Dy} | 72 | 45 | 56 | 55 | 12 | 54 | 0.970 |
| D_{Ho} | 57 | 39 | 48 | 47 | 10 | 46 | 0.958 |
| D_{Er} | 45 | 31 | 38 | 37 | 8 | 36 | 0.945 |
| D_{Tm} | 36 | 22 | 28 | 28 | 6 | 31 | 0.937 |
| D_{Yb} | 27 | 17 | 20 | 20 | 5 | 23 | 0.925 |
| D_{Lu} | 17 | 10 | 13 | 13 | 3 | 20 | 0.919 |
| D_{Hf} | 21 | 10 | 14 | 14 | 6 | n.d. | |
| D_{Ta} | 135 | 84 | 106 | 110 | 26 | n.d. | |
| D_{Pb} | 0.09 | 0.03 | 0.05 | 0.05 | 0.02 | n.d. | |
| D_{Th} | 2.5 | 1.39 | 1.9 | 1.9 | 0.50 | n.d. | |
| D_U | 1.42 | 0.94 | 1.1 | 1.1 | 0.27 | n.d. | |
| D_{Ra} | | | | | | <0.0001 | 1.44 |
| D_{Ac} | | | | | | 0.3 | 1.191 |
| D_{Pa} | | | | | | <1.3 | |
| R^2 | 0.9798 | 0.9220 | 0.9431 | 0.9470 | | | |
| ${}^{VII}E^{3+}$ (GPa) | 388 | 340 | 353 | 355 | 21 | 355 | |
| D_0 (M^{3+}) | | | | | | 74 | |
| ${}^{VII}r_0$ (M^{3+} ; Å) | | | | | | 1.016 | |

